13th World Conference on Earthquake Engineering
Vancouver, B.C., Canada
August 1-6, 2004
Paper No. 1085

SOME PROBLEMS ON THE SEISMIC DESIGN OF LARGE CONCRETE DAMS

Gao Lin [1], Zhi-qiang Hu[2], Shi-yun Xiao[2], Jian-bo Li[3]

SUMMARY

Some problems those are important for the seismic safety evaluation of large concrete dams against strong earthquake shocks are examined and discussed. First, based on the concept of viscoplastic consistency model, a modified four-parameter Hsieh-Ting-Chen viscoplastic model is developed to take account of the rate-dependent behavior of concrete. The earthquake response of a 278^{m} high arch dam has been analyzed, the results show that the strain rate affects the displacement and stress distribution to some extent. Second, a more accurate non-smooth Newton algorithm for the solution of three-dimensional frictional contact problems is developed to study the joint opening effects on the dynamic response of arch dams during strong earthquakes. The seismic response of two nearly 300^{m} high arch dam has been studied. It was found that canyon shape has great influence on the joint opening and the stress response of the dam. Third, the multi-transmitting boundary method and the damping-solvent method are used to carry out dam-foundation interaction analyses of arch and gravity dams. The foundation stiffness and foundation inhomogeneity on the dynamic stress response of the dam are examined and discussed. These findings help better understanding of the dynamic behavior of concrete dams and promote an improvement of the seismic design of arch and gravity dams.

INTRODUCTION

Many high concrete dams are being built in high seismic area - southwest part of China. These dams, such as the 292^{m} high Xiaowan arch dam, 278^{m} high Xiluodu arch dam, 305^{m} high Jinping arch dam may become highest in the world. The safety of these structures to resist earthquake shocks is of great concern. Despite the fact, that considerable progress has been achieved in the analysis techniques for dealing with earthquake engineering problems of concrete dams, many aspects essential for the safety evaluation of concrete arch dams as well as concrete gravity dams have not yet been well solved. The current practice in the earthquake-resistant design and seismic safety evaluation of concrete dams is based on the linear elastic analyses to a great extent. For the purpose to improve the seismic design of concrete dams, several problems which will deepen understanding of the dynamic behavior of concrete dams are examined and discussed.

[1] Professor of civil engineering, Dalian University of Technology, Dalian, China
[2] Doctor, Dalian University of Technology, Dalian, China
[3] Doctoral candidate, Dalian University of Technology, Dalian, China

Ⅰ.STRAIN-RATE EFFECTS

Most of the experimental studies have shown that concrete is sensitive to the rate of loading (Bischoff et al[1], Malvar et al[2]). The material strength, stiffness and ductility (or brittleness) of concrete are rate-dependent. Hence, when a dam is subjected to earthquake excitation, the stress-strain relationship exhibited in different parts of the dam at different instant will be different due to different strain-rate it experiences. However, in the conventional design practice the effect of rate-sensitivity is taken into account by means of drastic simplifying assumptions. That is, in spite of a wide variety of dam structures, the allowable stress of it under earthquake excitation is increased by, say, 30% of the value specified for static case. Similarly, the dynamic modulus of elasticity is assigned 30% higher than its static value. The effect of dynamic behavior of the dam and the effect of earthquake waveform on the strain-rate distribution of the structure has been disregarded. As a result, the true response of the dam may be altered to some extent. This problem has seldom been tackled in the current literature. Some researchers have studied the seismic response of two concrete gravity dams by employing rate-dependent damage model (Cervera et al[3], Lee et al[4]). Very few information concerning the effect of rate-dependency on the stress distribution and damage development has been obtained. In this paper, a consistency viscoplastic model is developed to investigate the strain rate effects on the seismic response of concrete dams.

Rate-dependent constitutive model of concrete

Wang[5] proposed a viscoplastic consistency model for analyzing mental, which can be seen as an extension of the classical-plastic approach to account for rate dependency. The model can relatively, easily be implemented in place of classical rate-independent plasticity models(Winnicki et al[6]). It is assumed, that during viscoplastic flow, the actual stress state must remain on the yield surface and satisfy the consistency condition. Thus, for viscoplastic loading, the yield surface is expressed by

$$f\left(\sigma_{ij},\kappa,\dot{\kappa}\right)=0 \text{ for } \dot{\lambda}>0 \tag{1}$$

where σ_{ij} is the component of stress tensor; κ is the internal variable and λ is the viscoplastic multiplier. The viscoplastic strain rate is defined as $\dot{\varepsilon}^{vp}=\dot{\lambda}m_{ij}$ and for associated flow rule $m_{ij}=\partial f/\partial\sigma_{ij}$. Thus, the yield surface is rate dependent and can change its size and shape according to the value of the viscoplastic strain rate. The consistency condition is formulated as

$$\dot{f}=\frac{\partial f}{\partial\sigma_{ij}}\dot{\sigma}_{ij}+\frac{\partial f}{\partial\kappa}\dot{\kappa}+\frac{\partial f}{\partial\dot{\kappa}}\ddot{\kappa}=0 \tag{2}$$

Assume that the rate of internal variable κ is a function of viscoplastic multiplier of the form $\dot{\kappa}=\dot{\lambda}g\left(\sigma_{ij}\right)$, the consistency condition becomes

$$m_{ij}\dot{\sigma}_{ij}-h\dot{\lambda}-s\ddot{\lambda}=0 \tag{3}$$

where *h* and *s* are the generalized plastic and viscoplastic modulus respectively.

$$h=-\frac{\partial f}{\partial\kappa}g\left(\sigma_{ij}\right),\quad s=-\frac{\partial f}{\partial\dot{\kappa}}g\left(\sigma_{ij}\right)$$

It has been shown that the model is capable of describing viscoplastic behaviour in an acceptable manner (Winnicki *et al* [6]). In this paper the consistency model concept is applied to the Hsieh-Ting-Chen four-parameter yield surface.

$$f\left(I_1,J_2,\theta\right)=aJ_2+(d\cos\theta+c)\sqrt{J_2'}+bI_1-1=0 \tag{4}$$

where I_1 and J_2 are the first invariant of stress tensor and second invariant of the stress deviator tensor respectively; *a*, *b*, *c* and *d* are material parameters determined by uniaxial and biaxial experiments. It is assumed that the two internal variables κ_t and κ_c separately corresponding to tension and compression

exist, so that the yield surface can change its shape due to separate hardening/softening processes of the compressive and tensile strength.

$$f_c = f\left(\sigma_{ij}, \kappa_c, \dot{\kappa}_c\right), \quad f_t = f\left(\sigma_{ij}, \kappa_t, \dot{\kappa}_t\right) \tag{5}$$

Based on the experimental results, it is assumed that

$$f_c = f_{c0} H_c\left(\kappa_c\right) R_c\left(\dot{\kappa}_c\right), \quad f_t = f_{t0} H_t\left(\kappa_t\right) R_t\left(\dot{\kappa}_t\right) \tag{6}$$

where f_{c0} and f_{t0} are the initial compressive and tensile strength respectively; $H_c\left(\kappa_c\right)$, $R_c\left(\dot{\kappa}_c\right)$, $H_t\left(\kappa_t\right)$, $R_t\left(\dot{\kappa}_t\right)$ are assumed functions that fit the experimental data as perfectly as possible. And the internal variable κ is taken as the equivalent viscoplastic strain.

$$\kappa = \bar{\varepsilon}^{vp} = \sqrt{\frac{2}{3}\varepsilon_{ij}^{vp}\varepsilon_{ij}^{vp}} \tag{7}$$

After some manipulation, finally the consistency condition becomes (Xiao,[7])

$$\frac{\partial f}{\partial \sigma_{ij}} d\sigma_{ij} + h d\lambda + s d\dot{\lambda} = 0 \tag{6}$$

$$h = a_c h_c(\kappa_c) R_c\left(\dot{\kappa}_c\right) + a_t h_t(\kappa_t) R_t\left(\dot{\kappa}_t\right)$$

$$s = a_c H_c(\kappa_c) r_c\left(\dot{\kappa}_c\right) + a_t H_t(\kappa_t) r_t\left(\dot{\kappa}_t\right)$$

where $h_c\left(\kappa_c\right) = \partial H_c / \partial \kappa_c$, $r_c\left(\dot{\kappa}_c\right) = \partial R_c / \partial \dot{\kappa}_c$, $h_t\left(\kappa_t\right) = \partial H_t / \partial \kappa_t$, $r_t\left(\dot{\kappa}_t\right) = \partial R_t / \partial \dot{\kappa}_t$

Solution of the problem is accomplished by an implicit backward Euler integration scheme, where the Newton-Raphson iterative procedure is employed. The calculated stress-strain relationships for uniaxial compression and tension by this model agreed fairly well with the experimental data.

Seismic response of an arch dam

In order to illustrate the effect of rate dependency on the dynamic structural response, the 278^{m} high Xiluodu arch dam in China subjected to earthquake excitation is analyzed by the proposed model. The material properties for the study are as follows: for the dam body E=2.4×10^{4}MPa, ν=0.17, ρ=2.4×10^{3}kg/m^3, static compressive strength f_c=30MPa, and static tensile strength f_t=2.5MPa; for the foundation rock E=1.6×10^{4}MPa, ν=0.25, ρ=2.0×10^{3}kg/m^3. Dynamic values of modulus of elasticity and strength are increased by 30%. Damping ratio of the dam and the foundation equals 0.05. The dam and the foundation are discretized into 450 and 1040 isoparametric elements respectively. Fig.1 shows the discretized dam-foundation system. An assumption of massless foundation is introduced to simplifying the dam-foundation interaction analysis though more rigorous interaction effects can be included. The design earthquake acceleration is 0.321g.

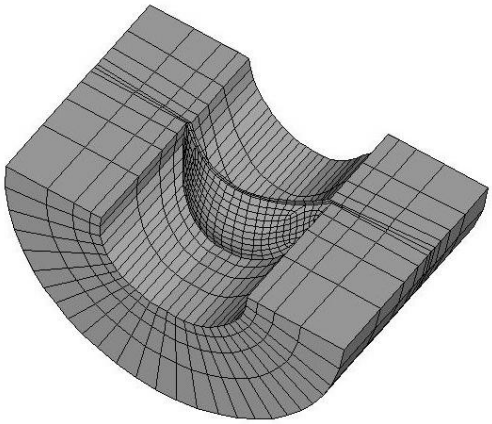

Fig.1 Geometry and mesh of arch dam.

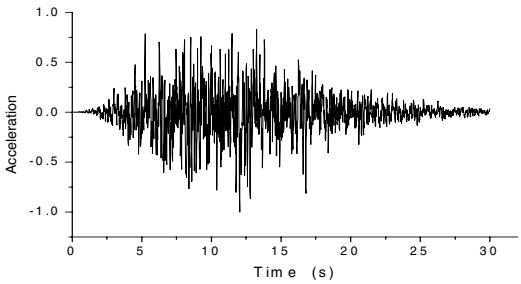

Fig.2 Time history of earthquake input

Three-component earthquake wave (2 horizontal, 1 vertical) is used as the input. Fig.2 shows the typical artificial acceleragram that meets the requirement of 《Chinese Specifications for Seismic Design of Hydraulic Structures》.

Three analyses were performed: an elastic analysis, a rate-independent plastic analysis and a rate dependent viscoplastic analysis. The static water pressure, the gravitational load and the earthquake load are included. The maximum values of the first and the third principle stresses in the dam in case of full reservoir are shown in Table 1. It is seen that in all three cases, the maximum compressive stress are nearly the same, the material remains working in the elastic range. However, referring to the maximum tensile stress there is marked difference between the calculated results of rate dependent model and that of rate independent model.

Table 1 Maximum values of principle stresses (High Level of Reservoir Water)

Model	Compression(MPa)	Tension(MPa)
Elastic	-12.15	5.80
Rate independent plastic	-13.15	3.46
Rate dependent viscoplastic	-13.10	4.48

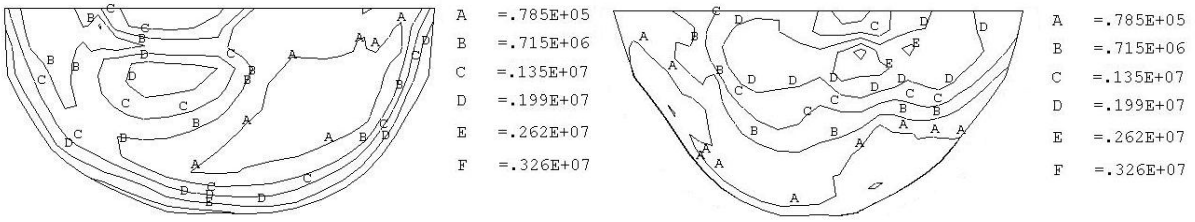

Fig.3 Distribution of first principle stresses (upstream and downstream face)
- rate dependent viscoplastic model (High reservoir water level)(Pa)

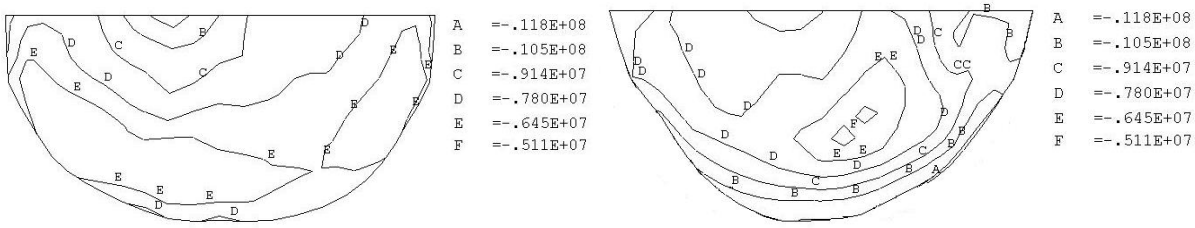

Fig.4 Distribution of third principle stresses (upstream and downstream face)
- rate dependent viscoplastic model (High reservoir water level) (Pa)

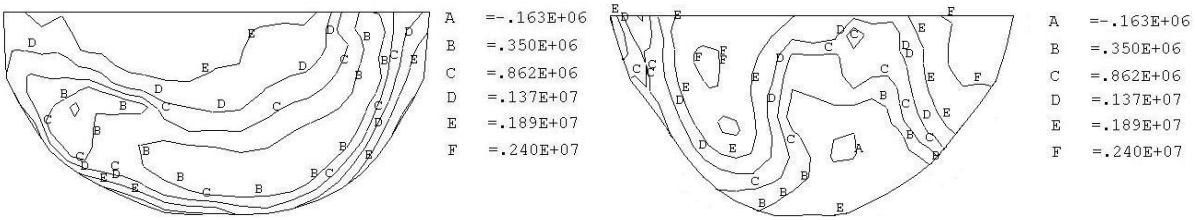

Fig.5 Distribution of first principle stresses (upstream and downstream face)
-rate dependent viscoplastic model (Low reservoir water level) (Pa)

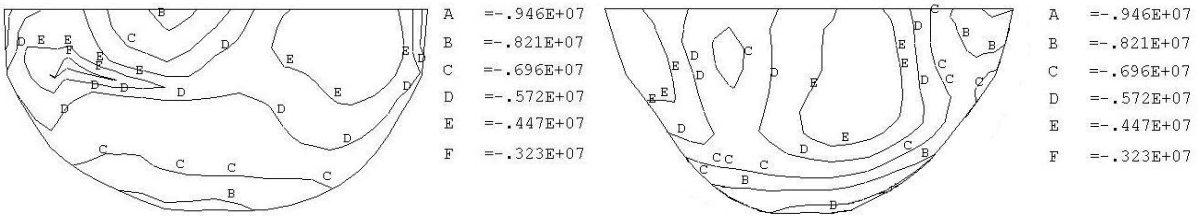

Fig.6 Distribution of third principle stresses (upstream and downstream face)
-rate dependent viscoplastic model (Low reservoir water level) (Pa)

Part of the numerical results are illustrated in Fig.3 to Fig.6, These results show that the stress distribution of rate dependent viscoplastic model and that of rate-independent viscoplastic model are very similar. Marked differences can be found between the stress distribution and strain-rate distribution in case if high reservoir water level and that in case of low reservoir water level.

The earthquake response of a 190^{m} high roller-compacted concrete gravity dam has also been examined by the rate-dependent and the rate-independent model. The dam is excited by a two-component earthquake wave with a design acceleration of 0.2g. The dynamic dam-foundation interaction effect is taken into consideration. In the analysis, the dead weight, reservoir water pressure, silt pressure, uplift pressure and the earthquake load are all included and the static load plays the dominant role. According to the "Chinese Specifications for Seismic Design of Hydraulic Structures", for the rate-independent model the elastic modulus of elasticity and the ultimate strength of concrete are increased by 30% of the value specified for the static case.

The calculated maximum horizontal displacement of dam crest increases from 0.161m for the rate-independent model to 0.174m for the rate-dependent model (Fig.7). With regard to the magnitude of maximum stresses and the stress distribution (Fig.8) over the dam surface no visible change can be found between the results of these two models. When rate-dependency is taken into consideration the maximum stresses rise in certain parts and decrease in another parts, the differences are kept within 0.3MPa. The strain rate distribution is given in Fig.9. The parts of high strain-rates not necessary coincide with the high stress parts. In case of earthquake excitation to specify the allowable stresses 30% higher than those of static case is not always on the safe side.

Fig.7 Envelops of maximum horizontal displacements(m)

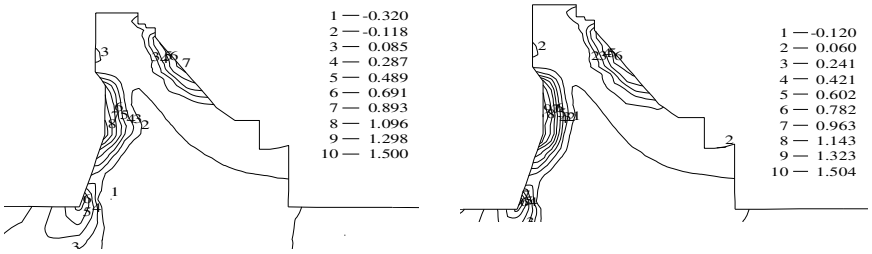

Fig.8 Envelops of maximum vertical stresses (MPa)

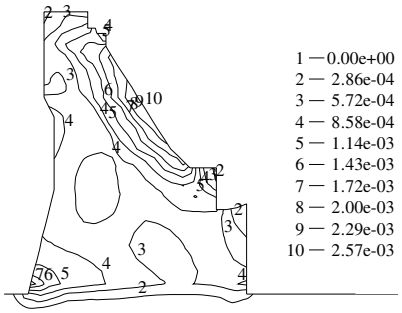

Fig.9 Distribution of maximum strain rates

II. JOINT-OPENING EFFECTS

The contraction joints of arch dam tend to open during strong earthquakes. The damage of Pacoima arch dam during 1971 San Fernando earthquake and 1994 Northridge earthquake provides evidence of such phenomenon. Weakening of dam integrity and causing damage to joint waterstops raise a safety concern to engineers when joint opening becomes significant. This is a kind of frictional contact problem characterized by highly nonlinear nature. Although a large number of algorithms for the numerical solutions of the related finite element equations and inequalities have been presented in the literature (Klarbring [9], Wriggers [10]), the problem is still under development. Considerable discrepancies exist from the results predicted by various algorithms. Fenves [11] first used a penalty approach to study the joint opening effects on earthquake response of arch dams. Based on the same approach Zhang et al [12] has analyzed the seismic response of 292^{m} high Xiaowan arch dam including the dam-canyon interaction effects. They compared the results of 1,3,5,7,9, and 21 joints, and they found that at least nine joints is necessary to simulate the joint opening effects of Xiaowan dam. Du et al [13] have also studied the number of joints and joint arrangement of Xiaowan arch dam on the accuracy of the simulated results. They indicated that the results obtained by penalty approach usually may not be sufficiently accurate and do not agree with the results of model experiments.

Summary of the analysis method

In this paper a non-smooth Newton algorithm is developed for the solution of frictional contact problems. The natural first order constitutive laws of contact and friction phenomena are reformulated as a nonlinear complementary system. Contact problems with friction are then entered as an application of the field of mathematical programming, which is based on sound mathematical principles and easily amenable to rigorous analysis. In general, global convergences of the solution can be ensured.

After finite element discretization the contact conditions are expressed in the form of nonlinear complementary equations. The unknown variables are taken as the vector of contact forces P and the increments of relative displacements Δu for the pair of nodes on two sides of the contact surface. The subscripts n, τ stand for normal and tangential component respectively, a and b stand for two perpendicular axes on the local tangential surface and the superscript i stands for the ith contact nodal pair.

(i) For normal contact and no penetrate conditions.

$$\min\left\{\Delta u_n^i, P_n^i\right\}=0 \quad , i=1,2,\ldots\ldots,NC\,, \qquad \Delta u_n^i \geq 0\,, \quad P_n^i \geq 0 \tag{9}$$

where NC is the number of nodal pairs.

(ii) For surface amenable to Coulomb's law of friction, the vector of contact force and the vector of increment of tangential relative displacement for the nodal pairs have the relationship

$$\min\left\{\Delta du_\tau^i, \mu P_n^i - P_\tau^i\right\}=0 \quad , i=1,2,\ldots\ldots,NC\,, \quad \Delta du_\tau^i \geq 0\,, \quad \mu P_n^i - P_\tau^i \geq 0 \tag{10}$$

where

$$\Delta du_\tau^i = \sqrt{\left(\Delta du_a^i\right)^2 + \left(\Delta du_b^i\right)^2} \quad P_\tau^i = \sqrt{\left(P_a^i\right)^2 + \left(P_b^i\right)^2}$$

Eq.(10) holds both for adhering and sliding state.

(iii)Under sliding state, the tangential force acts opposite to the direction of displacement. It may be written in the following form.

$$\arctan {P_a}/{P_b} = \arctan {\Delta du_a}/{\Delta du_b} + \pi$$

For simplifying the calculation, it is replaced by

$$\Delta du_a^i \sin\theta^i - \Delta du_b^i \cos\theta^i = 0 \tag{11}$$

where θ^i represents the angle between the direction of tangential contact force and the coordinate axis a. Eq.(11) shows that the tangential contact force and the sliding displacement lie on a same straight line, but they do not necessary act in opposite direction. Hence the following two sets of additional equations are formed.

$$\begin{gathered} P_a^i = P_\tau^i \cos\theta^i, \quad P_b^i = P_\tau^i \sin\theta^i \\ \Delta du_a^i = \Delta du_\tau^i \cos\left(\theta^i + \pi\right), \quad \Delta du_b^i = \Delta du_\tau^i \sin\left(\theta^i + \pi\right) \end{gathered} \tag{12}$$

Then, Eqs. (9),(10),(11) constitute the nonlinear complementary equations. P_n, P_τ and θ are the unknown variables, and $\Delta u_n, \Delta du_\tau, \Delta du_a$ and Δdu_b are nonlinear functions of the unknown variables. All contact forces and displacements should satisfy the equilibrium equations.

For ease of numerical solutions, Eqs. (9),(10),(11) and (12) are replaced by their equivalent set of nonsmooth equations (Chen W J et al [15])

$$\begin{cases} h_1^i = \min\left\{P_n^i, \Delta u_n^i\right\} = 0 \\ h_2^i = \Delta d\tilde{u}_\tau^i + \min\left\{0, \mu \max\left\{0, P_n^i - \Delta u_n^i\right\} + \tilde{P}_\tau^i - \Delta d\tilde{u}_\tau^i\right\} + \\ \qquad \max\left\{0, -\mu \max\left\{0, P_n^i - \Delta u_n^i\right\} + \tilde{P}_\tau^i - \Delta d\tilde{u}_\tau^i\right\} = 0 \\ h_3^i = \Delta du_a^i \sin\tilde{\theta}^i - \Delta du_b^i \cos\tilde{\theta}^i = 0 \end{cases} \quad i = 1,2,\ldots\ldots,NC \tag{13}$$

The new unknown variables now become $P_n, \tilde{P}_\tau, \tilde{\theta}$; correspondingly, $\Delta u_n, \Delta du_a$, $\Delta du_b, \Delta d\tilde{u}_\tau$ are functions of $P_n, \tilde{P}_\tau, \tilde{\theta}$. The contact conditions are perfectly satisfied and the system of equation (13) are solved by a generalized damped Newton method which involves solving in each iteration a possibly non-smooth system and performing a linear search which makes the method globally convergent. For dynamic problems the velocity and acceleration vector as well as the force vector for the pairs of contact nodes are modified such that the conservation of momentum and kinetic energy can be maintained when impact takes place.

The arch dam-foundation interaction effects are taken into consideration by the multi-transmitting boundary method in the time domain (Liao et al [16]). To ensure efficiency and stability of large scale numerical computation, an implicit-explicit integration scheme developed by Hughes et al [17] is implemented. It incorporates the advantages of predictor-corrector explicit integrator algorithm for the transmitting boundaries with that of Newmark integration scheme method for the solution of the equations of motion of the structures.

Seismic response of arch dams

The earthquake response of two high arch dams which are being built in China has been analyzed. The first one is the 278^{m} high Xiluodu arch dam, which has been analyzed in section I. The dam is located in a U-shaped canyon. The structure and the foundation is discretized into 99507 finite elements (107662 nodes for zero joint). The acceleration time history of Koyna earthquake with three-components is chosen as the input motion. The maximum horizontal acceleration is 0.321g. The earthquake waves excite

vertically upward from the bottom of the model. Cases with 0, 3, 5, 7, 9, 11 and 13 contraction joints have been studied (13 joints has 608 pairs of contact nodes). The arrangement of contraction joints along the dam axis is shown in Fig.11.

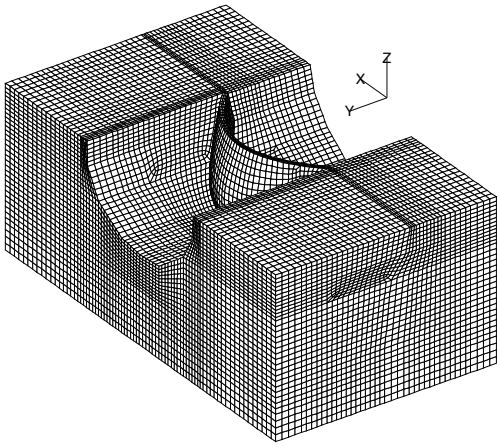

Fig.10 FEM model of dam-foundation system of Xiluodu arch dam

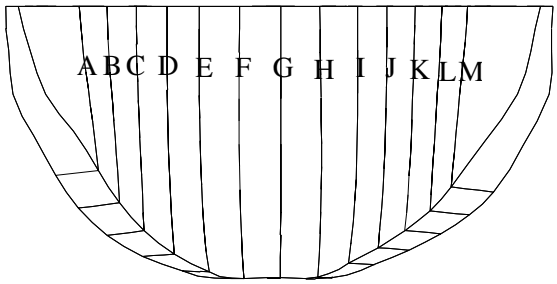

Fig.11 Arrangement of contraction joints of Xiluodu arch dam (downstream view)

In the calculation, the dead weight of the dam and the reservoir water pressure are included and the low operating water level (70^{m} below the dam crest) is used for the analyses. This reservoir condition is regarded as the most unfavorable case for the joint opening. Opening and sliding of the joints are allowed. The frictional coefficient between the contact concrete faces is assigned as 1.0. Cases where sliding is not allowed due to keying action produced by shear keys are calculated and compared in the second example. Table 2 and 3 show the maximum joint opening in the normal direction and maximum joint sliding in the tangential direction respectively.

Table 2 Comparison of maximum joint opening in the normal direction (cm)

case		A	B	C	D	E	F	G	H	I	J	K	L	M
3 Joints	U				1.2318			1.1872			0.9514			
	D				1.4765			1.1081			0.2694			
5 Joints	U	2.2857			1.3983			0.8804			0.7988			2.6609
	D	2.5471			1.6225			0.8188			0.3918			2.7465
7 Joints	U	1.9256		1.3610		1.3857		0.6824		0.4410		1.4104		2.0125
	D	2.0796		1.3526		1.4523		0.6011		0.3441		1.1652		2.2459
9 Joints	U	1.9363		1.2165		1.0609	0.5573	0.2906	0.2351	0.5318		1.2668		2.0778
	D	2.0649		1.1473		1.1349	0.6132	0.2980	0.2209	0.4720		1.0562		2.3106
11 Joints	U	1.9018		1.1104	0.542	0.8410	0.5666	0.2928	0.2255	0.3346	0.6738	0.9305		1.943
	D	2.0495		1.1437	0.6783	0.9365	0.6245	0.2985	0.2128	0.3405	0.4768	0.7093		2.1777
13 Joints	U	1.0587	0.8459	0.8185	0.5636	1.1205	0.6770	0.3060	0.2006	0.3162	0.7346	1.1573	0.9524	1.1037
	D	1.2152	0.8189	0.9206	0.7635	1.2656	0.7346	0.3277	0.2043	0.2467	0.5412	1.0896	0.8093	1.4153
7 Joints*	U	0.1995		0.3032		0.3533		0.6824		0.3424		0.3157		0.5273
	D	0		0.1809		0.3411		0.7538		0.3721		0.2555		0.3696

annotation: U-upstream face; D-downstream face; *-earthquake wave excits only in river direction.

Table 3 Comparison of maximum joint sliding in tangential direction (cm)

Case		A	B	C	D	E	F	G	H	I	J	K	L	M
3 joints	U				1.6279			2.2801			1.1519			
	D				1.635			2.3538			1.2571			
5 joints	U	5.2639			0.9770			2.2869			0.9593			6.1362
	D	5.2561			1.0141			2.4563			1.0149			6.1421
7 joints	U	4.4157		2.0193		1.4365		1.2754		0.6662		1.1794		5.6925
	D	4.3995		2.0009		1.4851		1.1155		0.6209		1.2164		5.5829
9 joints	U	4.1929		1.9487		1.1633	0.8888	0.7064	0.5710	0.7005		1.1887		6.3588
	D	4.155		1.9496		1.3075	0.9639	0.7755	0.5725	0.7563		1.2148		6.3708
11 joints	U	4.1036		1.9933	0.9019	0.7266	0.8654	0.6153	0.5297	0.5176	0.7967	1.1619		5.7318
	D	4.1079		2.0032	0.9278	0.8354	0.9337	0.6858	0.5323	0.5720	0.8444	1.1662		5.7218
13 joints	U	3.1199	1.9591	1.7862	1.2317	0.9936	0.8463	0.5493	0.4662	0.4176	0.5654	0.8908	2.5212	3.8773
	D	3.1231	1.8984	1.8168	1.2678	1.1039	0.6015	0.5777	0.4637	0.4567	0.6525	0.9593	2.5066	3.6791
7 joints *	U	0.4088		0.7680		0.4444		0.1022		0.5141		0.5036		2 . 4088
	D	0.2949		0.7958		0.4837		0.1092		0.5489		0.5332		2 . 2744

The joint opening and sliding along dam axis are demonstrated in Figs.12-13. Envelops of maximum major principle stress (tension) and maximum minor principle stress (compression) for cases with 13 joints and without joint are shown in Figs. 14 to 15.

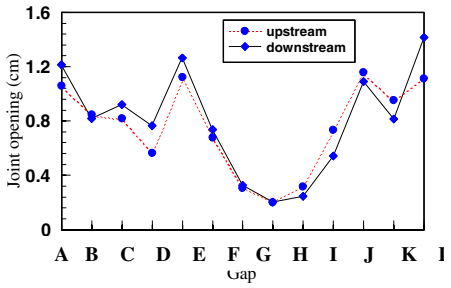

Fig.12 Joint opening along dam axis(Normal direction)

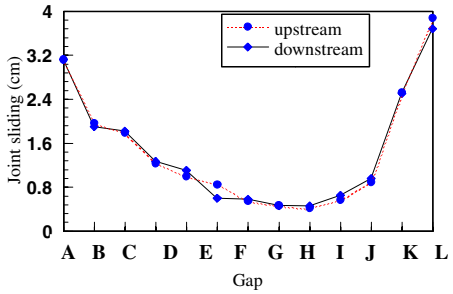

Fig.13 Joint sliding along dam axis (Tangential direction)

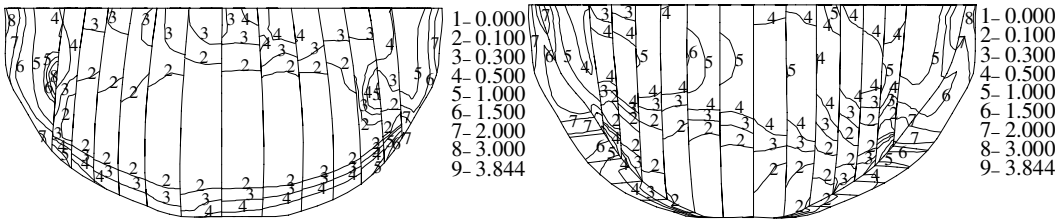

Upstream face Downstream face

Fig.14 Envelops of maximum major principle stress (13 joints model) (MPa)

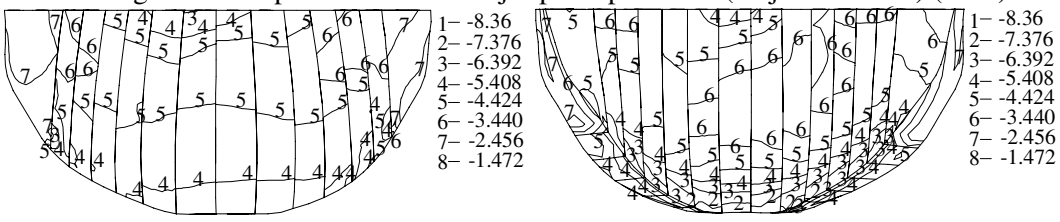

Upstream face Downstream face

Fig.15 Envelops of minimum major principle stress (13 joints model) (MPa)

The second example is the 292[m] high Xiaowan arch dam in a relatively wide V-shaped canyon. Material properties of the dam and foundation are: E_d=21GPa, ρ_d=2400kg/m^3, v_d=0.18; E_f=21GPa; ρ_f=2000kg/m$_3$, v_f=0.25. Reservoir water level is 59[m] below the dam crest. The same Koyna record is used as the earthquake input. The maximum design acceleration is 0.308g. The model is discretized into 117842 finite elements (126979 nodes for zero joint). Cases with 0, 3, 5, 9, 11 joints have been analyzed. The FEM model and the arrangement of contraction joints are shown in Figs.16-17. For comparison, a five-joint model where joint sliding is prevented by the keying action has also been analyzed.

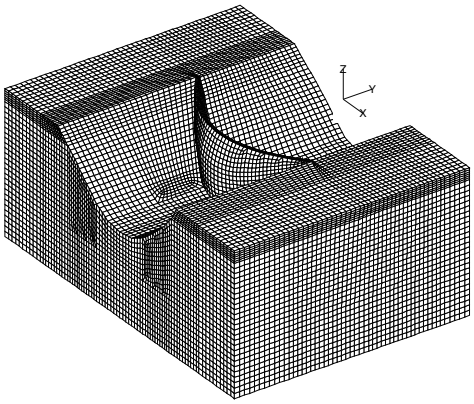

Fig.16 FEM model of Xiaowan arch dam

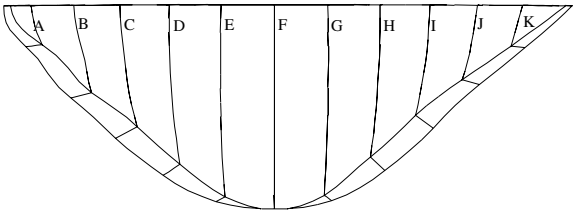

Fig.17 Joint arrangement of Xiaowan arch dam

Tabs. 4,5 show that maximum joint opening and sliding along the dam axis.
Envelops of maximum major and minor principle stress are shown in Figs.18-21 for the following two cases: (a) eleven-joint model; (b) five-joint model, where sliding is prevented.

Table 4 Comparison of maximum joint opening in normal direction (cm)

Case		A	B	C	D	E	F	G	H	I	J	K
3 joints	U			0.6849			1.2259			1.2951		
	D			1.1347			1.8848			1.1774		
5 joints	U		1.5867		0.3287		1.1062		0.8633		2.3172	
	D		1.607		0.3203		1.7771		0.6702		2.5027	
9 joints	U		1.3829	0.4310	0.4516	0.4585	0.9584	0.5355	0.8793	0.7608	1.4822	
	D		1.2565	0.3001	0.4137	0.5134	1.5062	0.9627	0.7865	0.7913	1.3519	
11 joints	U	0.8575	1.0061	0.4683	0.4613	0.4036	1.0395	0.6000	0.8586	0.7193	1.1736	1.0217
	D	0.9141	0.8925	0.3207	0.4230	0.3705	1.6136	1.102	0.7678	0.7415	1.0592	1.0752
5 joints*	U		1.853		0.273		0.973		0.485		2.738	
	D		1.843		0.011		1.748		0.371		2.789	

(annotation: * Joint sliding is prevented)

Table 5 Comparison of maximum joint sliding in tangential direction (cm)

case		A	B	C	D	E	F	G	H	I	J	K
3 joints	U			4.7311			3.1997			4.7885		
	D			4.6501			3.3892			4.8248		
5 joints	U		6.2663		2.1619		2.2786		2.5415		7.4648	
	D		5.8047		2.2906		2.4583		2.6318		6.49	
9 joints	U		7.0304	1.4239	2.1980	2.3683	1.9228	3.4715	1.738	1.7326	5.5158	
	D		6.5342	1.4777	2.3464	2.5459	2.0925	3.7378	1.804	1.671	4.6594	
11 joints	U	2.4832	6.4028	1.7103	2.1805	2.2209	1.9859	3.4883	1.740	1.7542	5.4308	2.3265
	D	2.138	6.9595	1.7675	2.3211	2.4017	2.1565	3.7812	1.8068	1.709	5.0276	2.1505

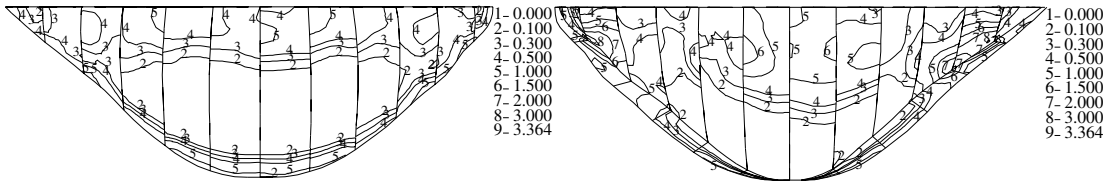

Upstream face downstream face

Fig.18 Envelops of maximum major principle stress (11 joint model) (MPa)

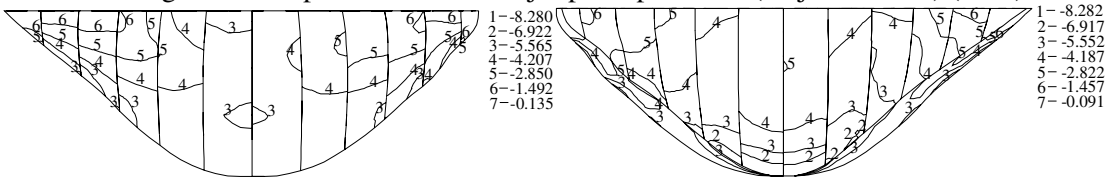

Upstream face downstream face

Fig.19 Envelops of maximum minor principle stress (11 joint model) (MPa)

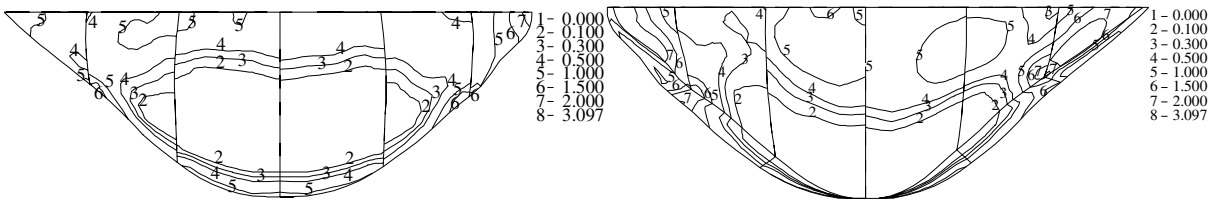

Upstream face downstream face

Fig.20 Envelops of maximum major principle stress (5 joint model – sliding prevented) (MPa)

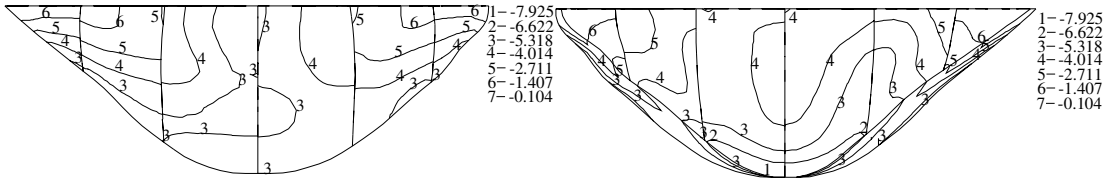

Upstream face downstream face

Fig.21 Envelops of maximum minor principle stress (5 joint model – sliding prevented) (MPa)

The results cited above lead us to the following conclusions:

(1) The greatest joint opening occurs usually at the crown section or quarter section of the arch in case the lowest vibration mode is an antisymmetric one.

(2)As the deformation of the abutment block is restricted by the canyon wall, the joints adjacent to the abutment block or its neighboring have the greatest value of slippage in the tangential direction. Particularly for the U-shaped canyon, this phenomenon becomes noticeable, the joint opening in the normal direction may also have very large value.

(3)Joint opening reduces dramatically the arch tensile stresses particularly in the center part of the dam, but it has insignificant effect on the cantilever stresses. Distribution of the minor principle stresses (compression) over the dam body for cases with and without joint opening are very similar. Discontinuity of stress contours take place when they across the joints.

(4) Great tendency of joint slippage in the tangential direction during strong earthquakes may cause the damage of shear keys and waterstops.

III. DAM-FOUNDATION INTERACTION EFFECTS

The dam-foundation interaction affects the earthquake response of dams in three aspects: (a) the foundation flexibility changes the vibration frequencies and vibration modes of the dam-foundation system; (b) the vibration energy of the system dissipates in the infinite medium of the foundation; (c) the earthquake input at the dam-foundation interface has been modified somewhat as compared with that of the free field. The dam-foundation interaction analysis is rather complicated and associated with large computational efforts, particularly for three-dimensional problems. To get a better understanding of the dam-foundation interaction effect, the variation of foundation stiffness on the seismic response of arch dams and gravity dams has been studied.

The arch dam considered here is a 102^{m} high double curvature dam with three centers located in a V-shaped canyon. The crest length is 310^{m}. the thickness of the crown section varies from 5^{m} at the crest to 24.6^{m} at the base. The dam-foundation system is descretized into 80476 finite elements (87180 nodes). Material properties of the dam are: dynamic modulus of elasticity E_d=28.6GPa, poisson ratiov_d=0.20, mass density ρ=2400kg/m^3. Three cases of foundation stiffness are examined, the ratio of foundation stiffness to dam E_f/E_d is chosen as 0.5, 1.0 and 1.5 respectively, which we may usually encounter in practice. Increasing foundation stiffness dramatically increases the computational effort. Earthquake wave of Koyna record excites only in river direction. The maximum acceleration is 0.20g. The dam-foundation interaction analyses are carried out by the multi-transmitting formula (Liao et al[16]). Figs.22-27 show the envelops of maximum major and minor principle stresses over the dam surface for these three cases. The distribution of stresses appear very similar; with regard to the magnitude of maximum stresses, it depends not only on the foundation stiffness, but may depend on a series of factors, such as the dynamic behavior of dam structure, the frequency content of earthquake wave, etc.

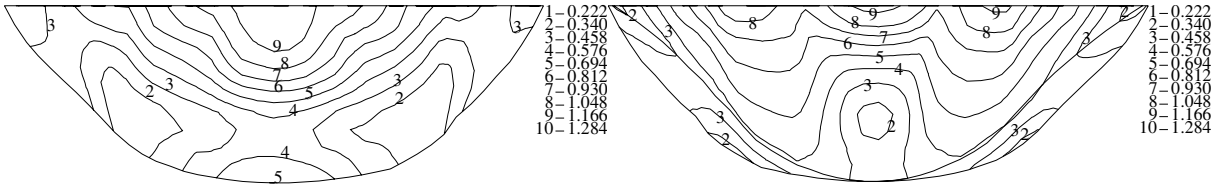

Fig.22 Envelops of maximum major principle stresses (upstream and downstream face)-case 1 E_f/E_d=0.5

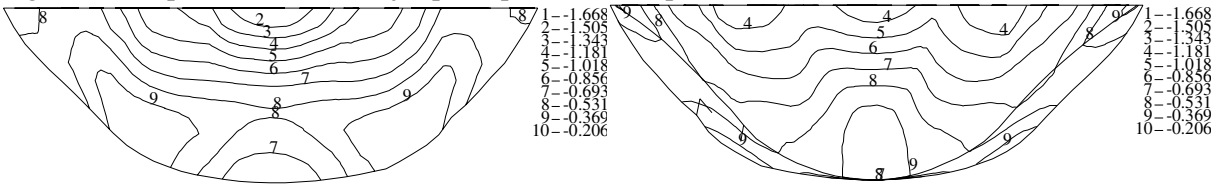

Fig.23 Envelops of maximum minor principle stresses (upstream and downstream face)-case 1 E_f/E_d=0.5

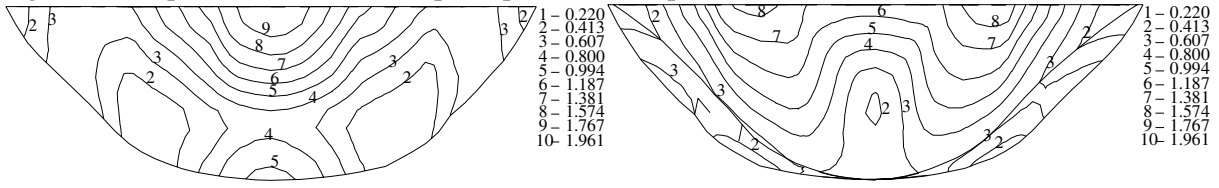

Fig.24 Envelops of maximum major principle stresses (upstream and downstream face)-case 2 E_f/E_d=1

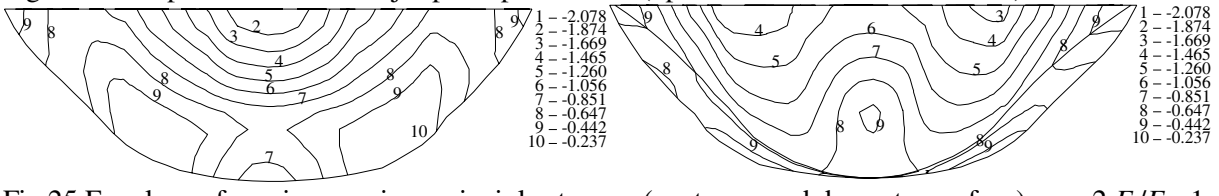

Fig.25 Envelops of maximum minor principle stresses (upstream and downstream face)-case 2 E_f/E_d=1

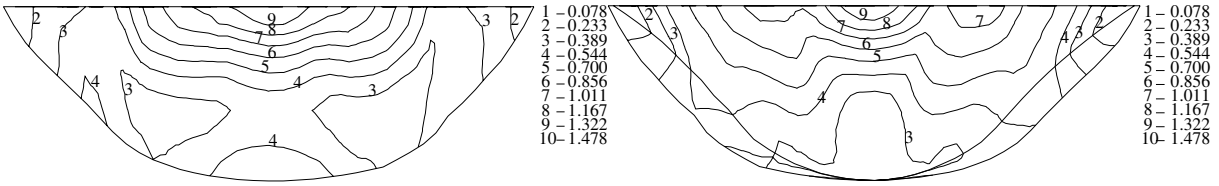

Fig.26 Envelops of maximum major principle stresses (upstream and downstream face)-case 3 E_f/E_d=1.5

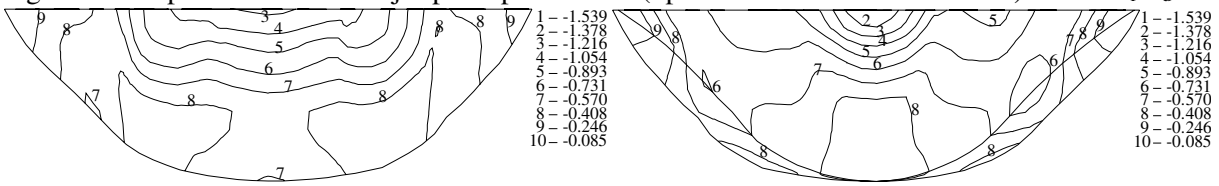

Fig.27 Envelops of maximum minor principle stresses (upstream and downstream face)-case 3 E_f/E_d=1.5

The 103[m] high Koyna dam is used to study the gravity dam-foundation interaction effects and it is excited by the Koyna earthquake in the horizontal direction with maximum acceleration of 0.38g. Material constants of the dam are assumed as E=30GPa, v=0.20, and ρ=2500kg/m^3. Based on the damping-solvent extraction method (Wolf et al[18]), a time domain sub-regional recurrence algorithm is developed (Li et al[19]) to carry out large scale numerical analyses of interaction problems. The dam and the foundation are discretized into 294 and 588 finite elements (330 and 645 nodes). Five cases have been studied: first three cases with foundation stiffness E_f/E_d=0.5, 1.0 and 2.0, the fourth case with foundation inhomogeneity in the horizontal direction, and the fifth case with foundation inhomogeneity in the vertical direction as shown in Fig.28.

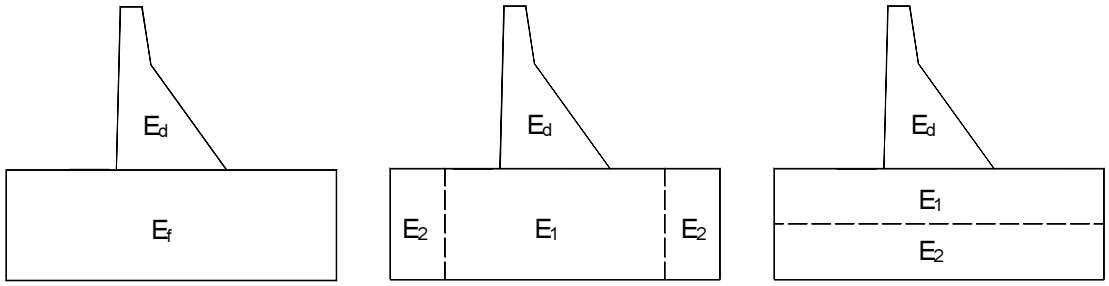

Case 1~3 Case 4 Case 5

Fig.28 Cases studied

Only the seismic stresses are taken into consideration. The maximum tensile stress response and the maximum compressive stress response are listed in Table 6. In addition, the maximum stress response for the massless foundation is also listed for comparison.

Table 6 Seismic stress response for Koyna dam (MPa)

		Case 1	Case 2	Case 3	Case 4	Case 5
		E_f/E_d=0.5	E_f/E_d=1.0	E_f/E_d=2.0	E_1=0.5E_d, E_2=E_d	E_3=0.5E_d, E_4=E_d
A	max. ten. stress	4.46	5.23	5.41	5.18	5.35
	max. comp. stress	4.02	4.51	4.01	4.53	4.54
B	max. ten. stress	9.18	6.61	6.32		
	max. comp. stress	7.87	5.09	5.52		

annotation: A- including dam-foundation interaction; B- massless foundation.

Envelops of maximum tensile stresses and compressive stresses are very similar. Fig.29 demonstrates the stress distribution of case 2.

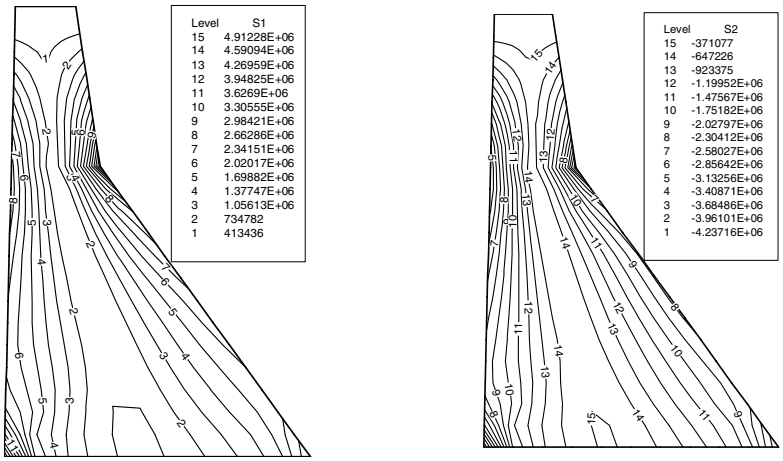

Fig.29 Envelops of maximum tensile and compressive stresses(E_f/E_d=1.0) (MPa)

The most vulnerable part is the neck section of the dam where slope of the downstream face changes. The results show that with the raising of foundation stiffness the maximum stresses response slightly increases. The foundation inhomogeneity affects the response to a certain extent, the inhomogeneity in the vertical direction plays more important role than the inhomogeneity in the horizontal direction. In comparison with the massless foundation the effect of dam-foundation interaction reduces the maximum stress response by about 15%~20% due to radiation damping. In case of foundation stiffness E_f/E_d=0.5, the maximum stress response of the massless foundation becomes much higher than the response when the foundation interaction effect is included. It is considered that the system may come to resonance with the exciting earthquake wave to some extent. Hence, in an exceptional case, the massless foundation may not give correct results.

CONCLUSION

As it has been noted above, the strain-rate effect of arch dam during strong earthquake and the dam-foundation interaction effect have great significance for the seismic response analyses of concrete dams. These problems should be paid attention to in the seismic safety evaluation of large concrete dams. Further improvement of the numerical analysis algorithm is needed.

ACKNOWLEDGEMENT

This research is supported by the National Science Foundation of China under grant No. 50139010.

REFERENCES

1. Bischoff PH, Perry SH. “Compressive behaviour of concrete at high strain rates.” Materials and Structures 1991, 24: 425-450
2. Malvar LJ, Ross CA. “Review of strain rate effects for concrete in tension.” ACI Materials Journal 1998; 95(6): 735-739
3. Cervera M, Oliver J and Manzoli O, “A rate-dependent isotropic damage model for the seismic analysis of concrete dams.” Earthquake Engng. Struct. Dyn. 1996, 25: 987-1010
4. Lee J, and Fenves GL. “A plastic-damage concrete model for earthquake analysis of dams.” Earthquake Engng. Struct. Dyn. 1998, 27: 937-956

5. Wang W. “Stationary and progressive instabilities in metals- a computational view” PhD, TU Delft, Netherlands, 1997.
6. Winnicki A, Pearce CJ, Bićanić N. “Viscoplastic Hoffman consistency model for concrete.” Computers and Structures 2001, 79: 7-19
7. Lin G, Xiao SY. “Seismic response of arch dams including strain-rate effects.” Proceedings of the International Conference on Advance and New Challenges in Earthquake Engineering Research, Ko JM, Xu YL , Editiors. Harbin and Hong Kong, 2002: 331-338
8. Chen J Y, Lin G, “Seismic response analysis of concrete gravity dam based on the strain-rate dependent damage model” (to be published)
9. Klarbring A. “Mathematical programming in contact problem.” Aliabdali MH, Brebbia C A, Editors. Computational methods in contact mechanics. Computational Mechanics Publications, Southampton, 1993: 233-263
10. Wriggers P. “Finite element algorithms for contact problems.” Arch. Compt. Mech. Engng. 1995, 2: 1-49
11. Fenves GL, Mojtahedi S, Reimer RB. “Parameter study of joint opening effects on earthquake response of arch dams.” Report No. UCB/EERC-92/05, Earthquake Engineering Research Center, College of Engineering, University of California at Berkeley, 1992
12. Zhang CH, Xu YJ, Wang GL, Jin F. “Non-linear seismic response of arch dam with contraction joint opening and joint reinforcements” Earthquake Engng. Struct. Dyn. 2000, 29: 1547-1566
13. Du XL, Tu J, Chen HQ, “Non-linear seismic response of arch dam-foundation systems with cracked surface.” Earthquake Engineering and Engineering Vibration (in Chinese), 2000, 20: 11-20
14. Hu ZQ, “Seismic Analysis of Arch Dams including effects of contraction joints and dam-foundation interaction.” PhD, Dalian University of Technology, Dalian, China, 2003
15. Chen WJ, Chen GQ, Feng EM. “Variational principle with nonlinear complementarity for three dimensional contact problems and its numerical method.” Science in China (A), 1996, 39(5): 528-539
16. Liao ZP, Wong HL. “A transmitting boundary for the numerical simulation of elastic wave propagation.” Soil Dynamics and Earthquake Engineering, 1984, 3: 174-183
17. Hughes TJR, Liu WK. “Implicit-explicit finite elements in transient analysis: stability theory.” J. Appl. Mech. 1978, 45(6):371-374
18. Wolf JP, Song CM. “Finite-element modeling of unbounded media.” John Wiley & Sons, 1996:217-251
19. Li JB, Chen JY, Lin G. “A sub-regional recurrence algorithm for solving dynamic soil-structure interaction problems in the time domain.” Engineering Mechanics (in Chinese) (to be published.)